Issues on the Use of Variogram-Based Feature Vectors in Content Based Image Retrieval

Zhixiao Xie and Fang Qiu

Introduction

Content Based Image Retrieval (CBIR) intends to objectively and efficiently retrieve interested images or image segments (pixel blocks) from a large-volume image database based on the content similarity between a query icon (or sample image) and database images (or image segments). CBIR was originated from computer vision and database community (Flickner et al., 1995; Pentland et al., 1996; Smith and Chang, 1996) and has been gradually accepted by GIScientists for geographic image database applications (Ma and Manjunath, 1996; Bruns and Egenhofer, 1996; Sheikholeslami et al., 1999; Agouris et al., 1999; Stefanidis et al., 2002; Bian, 2003; Bian and Xie, 2004).

To geographers, image retrieval is a reversal to image classification in regard to operational process since image retrieval starts with a content description and then identifies locations that contain the content. Image classification, on the other hand, begins with a study area and then identifies contents within the area. One key component in CBIR is to represent the semantic content of an image segment, often through a numeric index vector (called feature vector), with each element being a measurement of a visual property, such as color, texture, shape and so on. To represent the important spatial structure information within geographic images, approaches based on variogram has recently been adopted for CBIR (Huang et al., 1999; Aksoy and Haralick, 2000; Bian and Xie, 2004). While the concept of variogram

Zhixiao Xie is an assistant professor in the Department of Geosciences at Florida Atlantic University. Fang Qiu is an assistant professor in the Program in Geographic Information Systems at the University of Texas at Dallas.

Figure 1. Illustrate how to determine whether two sample points (O, A) are location pairs separated by a lag d along a direction θ, defined by a distance tolerance (td), a direction tolerance (α), and a band-width (b).

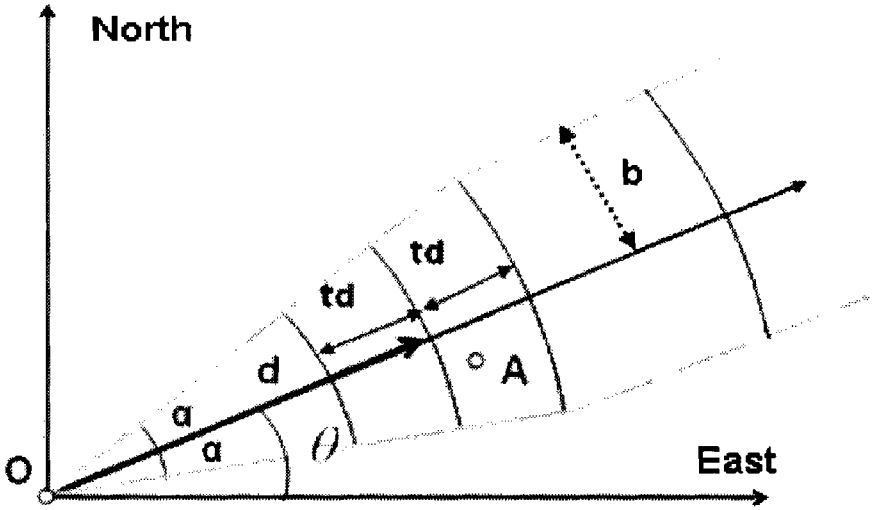

is not new, some important aspects require further study to ensure these approaches be properly applied in CBIR. This paper examines several issues in this regard.

Variogram

Variogram is a key concept underlying a set of spatial interpolation approaches called Kriging in geostatistics (Issaks and Srivastava, 1989). Like many spatial interpolation methods, the objective of Kriging is to interpolate a continuous surface from a limited number of sample points. In an image, the pixel centers are normally regarded as the nominal sample point locations. It is from these sample points that empirical variograms are constructed and used for subsequent inference.

A variogram (or more formally, semi-variogram) is a plot of semi-variance vs. lag distances, where the spatial continuity or the association between semi-variances and the lag distances is explicitly presented. The association may show directional difference, representing

spatial continuity anisotropy, and the anisotropy can be characterized by the differences of variograms along different directions. In geostatistics, a semi-variance $\gamma(h)$ is commonly calculated as the average of the squared difference of values of a variable at paired locations separated by a lag distance h, and along a specific direction θ (Eq. (1)).

$$\gamma(h) = \frac{1}{2N}\sum\left(V_s - V_{s+h}\right)^2 \tag{1}$$

where, V_s and V_{s+h} are the values of a variable at two locations separated by a lag distance h; N is the number of such location pairs. To construct a useful variogram, a sufficient number of sample location pairs for each lag distance are required, since too few pairs may give a variogram too erratic to serve as a useful description (Issaks and Srivastava, 1989). However, in many cases, sample location pairs may not be separated exactly by a distance used for a lag and along a direction needed in the variogram plot. Therefore, a tolerance for distance (td) and a tolerance for direction (α) are often used to determine whether two (set of) sample locations could be paired for a lag (Fig. 1). For example, although OA is not exactly separated by a lag distance d, along a direction θ, OA is still considered as a location pair separated by a lag distance d, because A falls within the area defined by distance and directional tolerances. Obviously, the areas defined by tolerances for two neighboring directions may overlap, causing some location pairs to be used for more than one direction, which will possibly blur some directional differences (Deutsch and Journel, 1997). Therefore the overlap should be carefully reduced. Further, a bandwidth b may be applied as well to further decrease the blurring effects (Fig. 1).

In Kriging, after the empirical variograms have been calculated from sample locations, they are usually fitted with theoretical models, most commonly spherical, exponential or Gaussian. These theoretical models are later used to derive the weights of sample locations for interpolating values at un-sampled locations. However, application of variograms in CBIR is somehow different.

Variograms applied in CBIR

Variograms have been used to capture textual information for CBIR (Huang et al., 1999; Aksoy and Haralick, 2000; Xie, 2004) and for remote sensed image classification (Curran, 1988; Miranda et al., 1992; Lark, 1996; St-Onge and Cavayas, 1995; Wallace et al., 2000, Carr, 2002; Jensen, 2004). An intuitive approach for adopting variograms in these contexts is to use the key parameters of the theoretic variogram models, such as nugget, range and sill, as the texture and structure descriptors. Although this approach was applied in image classification (St-Onge and Cavayas, 1995; Wallace et al., 2000), it is considered not applicable in CBIR at present, because a CBIR requires a highly automated process, while it is still not reliable to automatically fit empirical semivariograms with theoretical models (Atkinson and Lewis 2000).

A more feasible approach in CBIR up to now is to bypass the curve fitting bottleneck and construct feature vectors with elements being a set of semi-variances, calculated from a set of selected lags and directions. For example, Aksoy and Haralick (2000) compute the gray level variances for 5 different distances and 4 directions, and an image is represented with a vector of 20 variances (their research is not strictly variogram-based, but closely related). Huang et al. (1999) use color correlogram to capture the spatial correlation of color pairs over certain distances. Algorithms for effectively dealing with rotated or flipped spatial anisotropy phenomena, which are common rather than accidental in geographic images, are proposed by Xie (2004). However a couple of issues should be paid more attention in using this approach as discussed below.

The determination of location pairs

First, when calculating semivariances, it is essential to determine appropriate location pairs, which are separated by a lag distance and along a direction in an image segment. If a feature vector needs to characterize the spatial continuity anisotropy commonly existing in geographic images, the semivarainces should be calculated along sufficient number of directions. Further, geographic images may capture similar geographic entities at different orientations or the entities may be rotated/flipped relative to each other in different images (Fig. 2).

Figure 2. Illustration of the common situation that similar geographic objects in images are oriented differently.

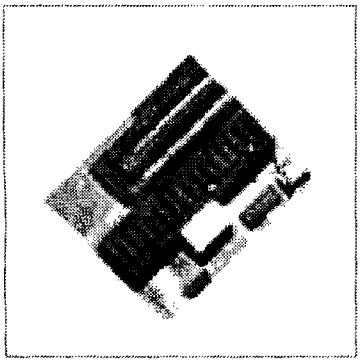

In order to reach a rotation/flip invariant comparison (Xie, 2004), it is essential that the same set of lag distances be used for different directions.

As a common sense, pixels are arranged in a regular spatial grid in an image, and it is not a challenge for appropriate pair location determination if only horizontal and vertical directions, (i.e. 0 ° and 90°) are considered. If we assume the pixel size is fixed and denote it as one unit, for either horizontal or vertical direction, a set of lag distances can be easily selected at the integer number of such units, k, (k ranges from 1 unit to one thirds or a half of the segment size). By selecting lags in such a way, it is guaranteed that a sufficient number of location pairs will be available. Moreover, no tolerances are necessary since the lags cover the exact distances between pixel centers, and the exact samples locations and values are used.

Unfortunately, we need more than these two directions in many cases, and issues may arise when dealing with diagonal (45° and 135°) and other directions such as 22.5° and so on. Along diagonal directions, the distance between two pixel centers is $\sqrt{2}k$ units. It means that a common set of lag distances along diagonal directions and horizontal / vertical directions are not readily available given the existing sample locations. A tolerance on lag distance may have to be used when determining location pairs if we want to use the same set

of lags (k units) as those readily available along horizontal /vertical directions. A directional tolerance is not necessary because a lag tolerance is enough for producing sufficient pairs. In fact, this can also avoid blurring directional differences due to unnecessary directional tolerances. To ensure each sample location (a pixel center) have a meaningful corresponding location for any lag distance (k units), the lag tolerance should be $\frac{1}{2}\sqrt{2}$ units, which is the largest distance from an un-sampled location to a sample location (pixel center). In cases when two candidate sample locations are within the tolerance range, it is preferable to pick the one closer to the location with exact lag distance.

For other directions other than diagonal, horizontal, and vertical, both a directional tolerance and lag distance tolerance are needed since very rarely can we find sufficient location pairs if only a lag distance tolerance is used. Many software packages are available for calculating variograms by setting directional/lag distance tolerances, such as VARIOWIN (Pannatier, 1996), GSLIB (Deutsch, and Journel, 1997), and the Geostatistical Analyst Extension in ArcGIS by ESRI. However, an unanswered yet important question is what tolerances are reasonable for extracting variogrms along arbitrary directions in images. In geostatistics, the principle for setting directional tolerance is to use as small an angular tolerance as possible to limit the blurring anisotropy effect that results from combining pairs from different directions (Issaks and Srivastava, 1989). As illustrated in Fig. 3, for any direction, an angular tolerance of 22.5° should be sufficient since a sample location (pixel center) can definitely be found within the area defined by such a directional tolerance for any lag distance. To minimize blurring further, a bandwidth (b) should be set at $\frac{1}{2}\sqrt{2}$ units, because this is half the maximum distance between two neighboring pixels ($\sqrt{2}$ units) and at least one sample location can be found for any lags (k units). For the similar reason, the lag distance tolerance can also be set at $\frac{1}{2}\sqrt{2}$ units.

Figure 3. An illustration of the distance tolerance (*td*), directional tolerance (α), and bandwidth to be used for determining location pairs along directions other than horizontal, vertical and diagonal. Specifically, $\alpha = 22.5°$, $td = b = \frac{\sqrt{2}}{2}$ units, $L = \frac{b}{\sin(\alpha)} - \left(\frac{\sqrt{2}}{2}\right) \Big/ \sin(22.5°)$ units. L denotes when the bandwidth starts to play a role.

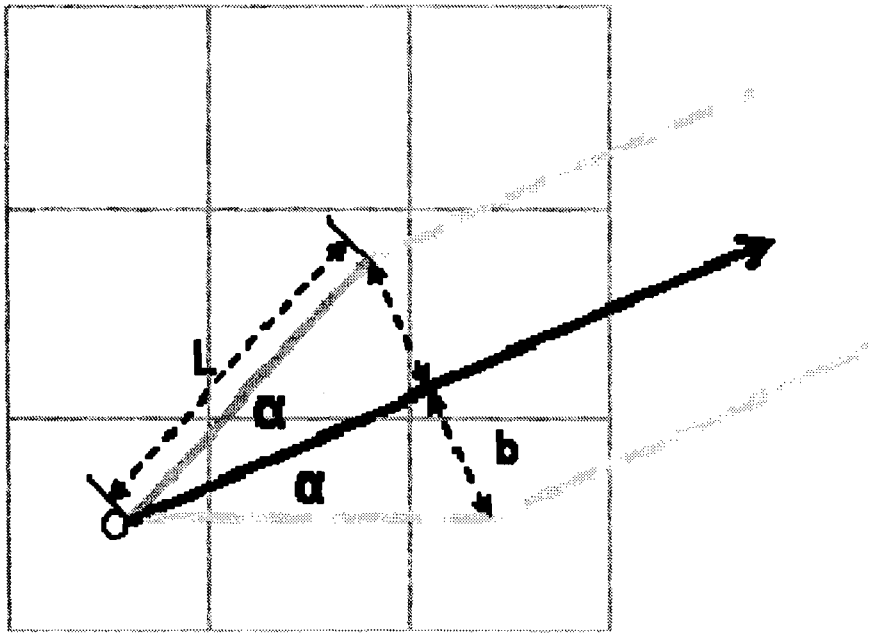

In the above discussions, we implicitly measure lags using Euclidean distance metric. This is necessary since variograms characterize spatial continuity, which states that things nearer in space tend to be more similar than those farther away from each other, and the concept of "near" or "far" should be measured with Euclidean distance in most cases. However, in some related applications (Huang et al., 1999; Aksoy and Haralick, 2000), a distance metric (Eq. (2)) has often been misused due to its implementation simplicity.

Figure 4. An image segment with isotropic spatial pattern (a), and the directional variograms (b) along two directions, 0° and 45°, using the $d = \max\{|r_1 - r_2|, |c_1 - c_2|\}$ as the distance metric for lags.

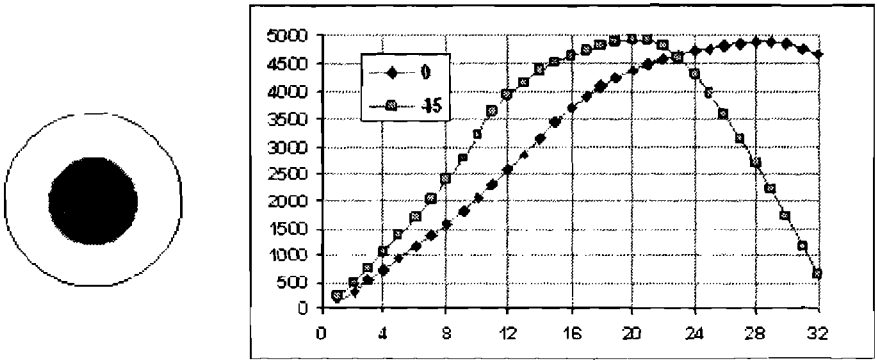

$$d = \max\{|r_1 - r_2|, |c_1 - c_2|\} \tag{2}$$

where, (r_1, c_1) and (r_2, c_2) are the rows and columns of two pixels.

Apparently in any non-horizontal and non-vertical directions, the distance between the two pixel centers are $\sqrt{(r_1 - r_2)^2 + (c_1 - c_2)^2}$ units in Euclidean distance, and $\sqrt{(r_1 - r_2)^2 + (c_1 - c_2)^2} > \max\{|r_1 - r_2|, |c_1 - c_2|\}$. As a result of using this distance metric (Eq. (2)), some semi-variances (or variances) in non-horizontal and non-vertical directions will be mistakenly associated with a shorter lag, as will inevitably distort the actual spatial continuity present in the image object.

Such distortions are illustrated in the two directional variograms in Fig. 4. These two variograms are computed based on the image segment in Fig. 4a, one along 0° direction and the other 45° (Fig. 4b). Although there exist no directional differences in spatial continuity in the original image object, the variogram curve along the 0° direction is completely different than that along the 45° direction when the lag

Figure 5. A series of image segments containing disc objects of varied sizes. The size of a pixel is 1 unit of distance and the diameters of the internal discs are 8, 16, 24, 32, 40, 48, 56 units for a_1 to g_1 and a_2 to g_2, respectively. 1) The size of all square segments is 64 by 64 units. 2) The diameter of all circle segments is 64 units.

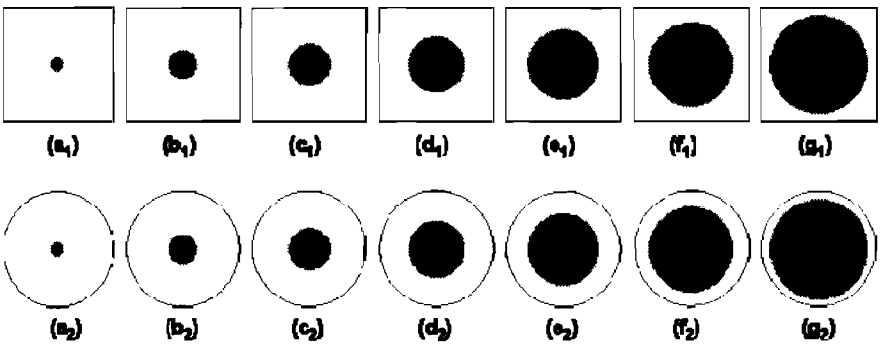

is measured using the metric in Eq. (2). Consequently, Euclidean distance should always be adopted to measure lag distances to avoid directional distortion.

The image segment shape

In CBIR, an image is often subdivided into small image subsets, also referred to as image segments. The calculation of semi-variances is conducted for each image segment. A square shape is often chosen for convenience. However, the appropriateness of using the square shape has not been carefully examined or explicitly justified. In this section, we investigate the benefits and drawbacks of two different segment shapes, squares and circles.

To compare the different effects exerted by square and circle shaped image segments on the resulting variograms, two experiments are conducted based on hypothetical image segments. The first experiment involves the use of a series of discs of varied sizes centered in square (Fig. $5a_1$-g_1) and circle (Fig. $5a_2$-g_2) image segments. The use of discs is based on the consideration that a disc bears no directional differences in spatial continuity and exhibits spatial isotropy. In theory, the variograms derived from an image segment containing a disc should be the same or at least sufficiently close in all directions. An ideal image segment shape should be the one that faithfully char-

acterizes the spatial isotropy of a disc object.

The size of each square image segment in Fig. $5a_1$-g_1 is 64 by 64 units of distance (in Euclidian distance metric) and the diameter of each circle segment in Fig. $5a_2$-g_2 is 64 units. The diameters for the center discs are 8, 16, 24, 32, 40, 48, 56 units as shown in Fig. $5a_1$ to $5g_1$ and $5a_2$ to $5g_2$ respectively. In all the image segments, the DN value is 127 for the white pixels and 0 for the dark pixels.

For each of the image segments in Fig. 5, we calculate variograms along 8 directions, including 0°, 22.5°, 45°, 67.5°, 90°, 112.5°, 135°, and 157.5°, and at lags from 1 to 64 units . The resulted variograms from using the square segments and circle segments are shown in Fig. $6a_1$ to $6g_1$, and $6a_2$ to $6g_2$, respectively.

As shown in Fig. 6, no matter what image segment shape is adopted, variograms obtained from discs of varied sizes demonstrate similar overall patterns along the same direction, although the ranges and sills change with the size of the discs. However, the variograms along different directions become significantly dissimilar when the square segment (Fig. $6a_1$-g_1) is applied, no matter what size disc is contained. The variogram curves along diagonal directions (i.e. 45° and 135°) exhibit the largest deviations from those along horizontal and vertical directions (i.e. 0° and 90°), whereas the variogram curves along 22.5°, 67.5°, 112.5°, and 157.5° fall in between. In comparison, the circle segments produce almost identical variograms for all directions for each segment, though subtle discrepancies do exist (Fig. $6a_2$-g_2).

The second experiment assesses how the shape of an image segment affects the directional variograms for image segments containing an anisotropic object, a rectangle in this case. Unlike a disc, a rectangle exhibits directional differences in spatial continuity (i.e. spatial anisotropy). In order to assess the sensitivity of a variogram to the various rotated versions of an object, the same rectangle is oriented at two different angles (i.e. 0° and 45°), embedded within both the square and circle image segments. A segment shape is regarded as more appropriate if the variograms derived from the same object with different orientations are still sufficiently close with regard to the object directions.

Figure 6. The empirical variograms along 8 directions (0°, 22.5°, 45°, 67.5°, 90°, 112.5°, 135°, 157.5°, and the angle is measured counter-clockwise starting from due east), and at lags from 1 to 64 units of distance using both square segments (a_1-g_1), and circle segments (a_2-g_2).

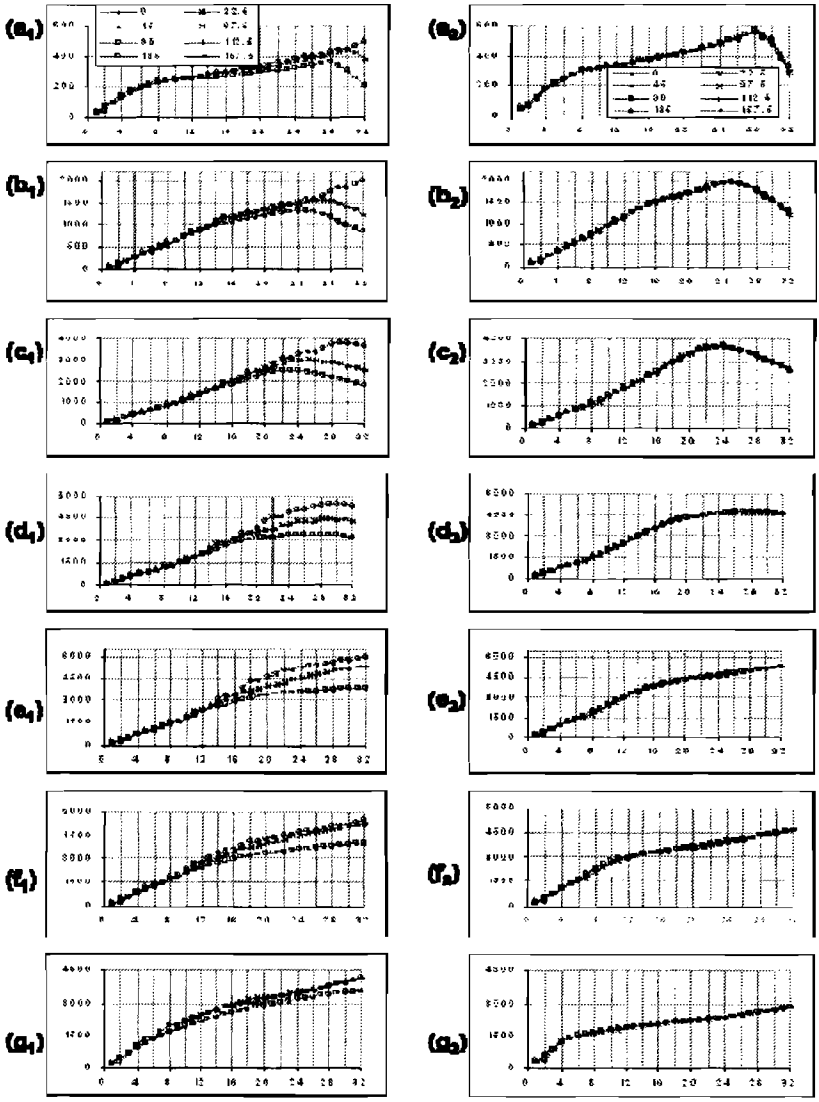

Figure 7. The same rectangle object within square image segments (SO, SR) and circle image segments (CO, CR). The rectangle objects in SO and CO are of original orientation (i.e. 0° rotation), while those in SR and CR are rotated at 45° counter clockwise.

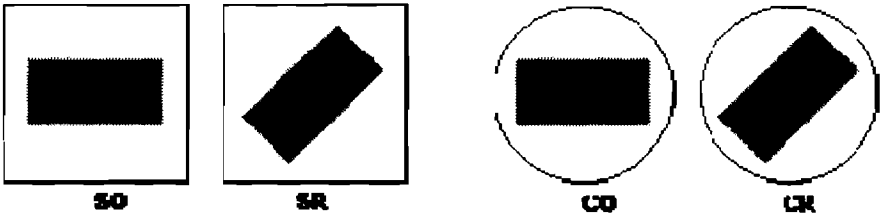

This experiment analyzes a set of 4 image segments, each containing the same 48 by 24 unit rectangle (Fig. 7). Again, the DN value for the white pixels is 127 and that for the dark pixels is 0. Two of the 4 segments are square-shaped with a dimension of 64 x 64 units (Fig. 7-SO and SR) and the other two are circle-shaped with a diameter of 64 units (Fig. 7-CO and CR). The rectangle objects in Fig 7-SO and CO are of original orientation (i.e. 0° rotation), while those in Fig 7-SR and CR are rotated at 45° counter clockwise.

The resulted variograms for the image segments in Fig. 7-SO and SR are shown in Fig. 8a, and those for the image segments in Fig. 7-CO and CR are displayed in Fig. 8b. For the image segments in Fig. 7-SO and CO, five directional variograms at 0°, 22.5°, 45°, 67.5° and 90° of angles are produced. For those in Fig. 7-SR and CR, five corresponding directional variograms at 45°, 67.5°, 90°, 112.5° and 135° of angles are created, because the rectangle objects in these later two image segments are rotated 45°. When the square segments are used, the variograms for the two different object orientations (i.e. Fig 7-SO and SR) along the corresponding directions (e.g. 0° in SO and 45° in SR) are significantly different from each other (Fig. 8a). Conversely, variogram curves for the corresponding directions are almost identical when the circle segments are used (Fig. 8b).

A preliminary conclusion can be made based on above discussions. To describe spatial continuity, circle segments are able to truthfully characterize both isotropic and anisotropic continuity information of objects in the image segments, as illustrated in the two experiments.

Figure 8. The directional variograms for the image segments in Figure 7. (a) Variograms for Fig. 7-SO and SR, where x-SO and x-SR denotes x° directional variogram for the image segments containing original and rotated objects respectively. (b) Variograms for Fig. 7-CO and CR, where x-CO and x-CR stands for x° directional variogram for the image segments containing original and rotated objects respectively.

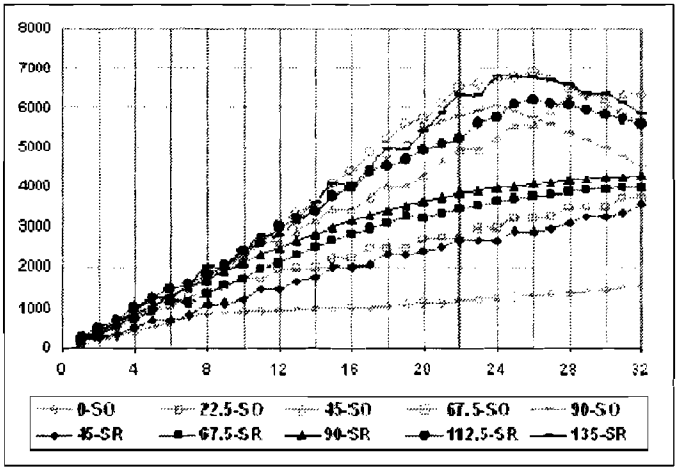

(a)

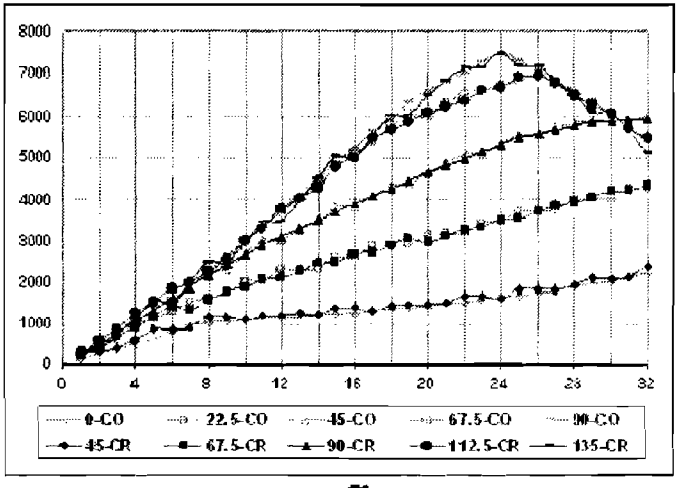

(b)

Figure 9. Four image segments with the same spatial structure, i.e. each containing a disc object of the same size (32 units in diameter). The DN values for all the dark pixels in the disc are 0. The DN values for the shaded pixels outside the disc vary from 15, 31, 63, and 127 for segments (a) to (d), respectively.

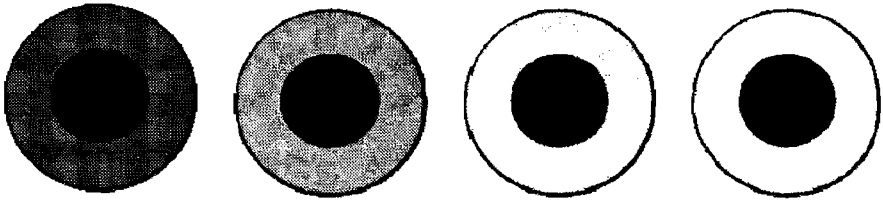

On the contrary, square segments may distort the spatial continuity of both isotropic and anisotropic image objects, due to the anisotropic nature of the square shape in itself. Other non-circle segments may also lead to similar distortions for the same reason. Therefore circle segments are believed by the authors to be more appropriate for deriving variograms from a remotely sensed image.

The relative semivariogram

All the variograms we have examined so far are absolute variograms, in which the actual semi-variances of the DN values are used to construct variogram curves. The absolute semivariances may depend on the mean of data values for that lag. In geostatistics, relative variograms are used to take account of the changing mean and to scale semivariances so that a clearer description of the spatial continuity can be produced (Isaaks and Srivastava, 1989). In this section, we evaluate whether relative variograms are a better alternative when spatial structure is of primary concern instead of DN value variances in CBIR.

To this end, we create a set of 4 circle image segments (64 units in diameter) with similar spatial structures, all containing an disc at the segment center with a diameter of 32 units (Fig. 9). Within each image segment, the DN value for the dark pixels of the internal discs is 0, but the DN value for the shaded pixels (ranging from dark gray to white) outside the internal disc varies from 15, 31, 63, to 127 as

shown in Fig. 9a-d respectively.

There are several types of relative variograms: local relative variograms, general relative variograms, and pairwise relative variograms. Both general and pariwise relative variograms can provide adequate display of spatial continuity (Isaaks and Srivastava, 1989). Detailed comparison of the two are beyond the scope of this paper and only pairwise relative variograms are used to present the concepts here.

The pairwise relative variogram adjusts the variogram calculation by a squared mean, and the adjustment is done separately for each pair of samples, as shown in Eq. (3).

$$\gamma(h) = \frac{1}{2N} \sum \frac{(V_s - V_{s+h})^2}{\left(\frac{(V_s + V_{s+h})}{2}\right)^2} \qquad (3)$$

where all the variables, including V_s and V_{s+h}, carry the same meaning as in Eq. (1).

For comparison purposes, we also calculate the absolute variograms for the 4 image segments in 8 directions, using Eq. (1). The resulted absolute and relative directional variograms are displayed in Fig. 10a and 10b respectively. The curves of the absolute variograms are dramatically different for the 4 image segments (Fig. 10a) with the semi-variance at the same lag increasing with the increasing DN values of the shaded pixels outside the internal disc (i.e. 15, 31, 63 and 127 respectively). In comparison, all the relative variograms are remarkably similar to each other as shown in the Fig. 10b, independent of the DN value variation.

To quantitatively document the differences between the set of absolute variograms and between the set of relative variograms, we further calculate the mean and the standard deviation of all the absolute and the relative semi-variances over each lag. The ratio (%) of the standard deviation to the mean is then derived in order to show the magnitude of overall deviation from the mean semi-variance at each lag. Fig. 11a displays the ratio values derived from both the absolute and relative semi-variances in the same plot. Fig. 11b presents only

Figure 10. The absolute variograms (a) and relative variograms (b) for the image segments in Figure 9, where A-x, B-x, C-x, and D-x represent the directional variograms in x° direction for image segments in Fig. 9a-d respectively.

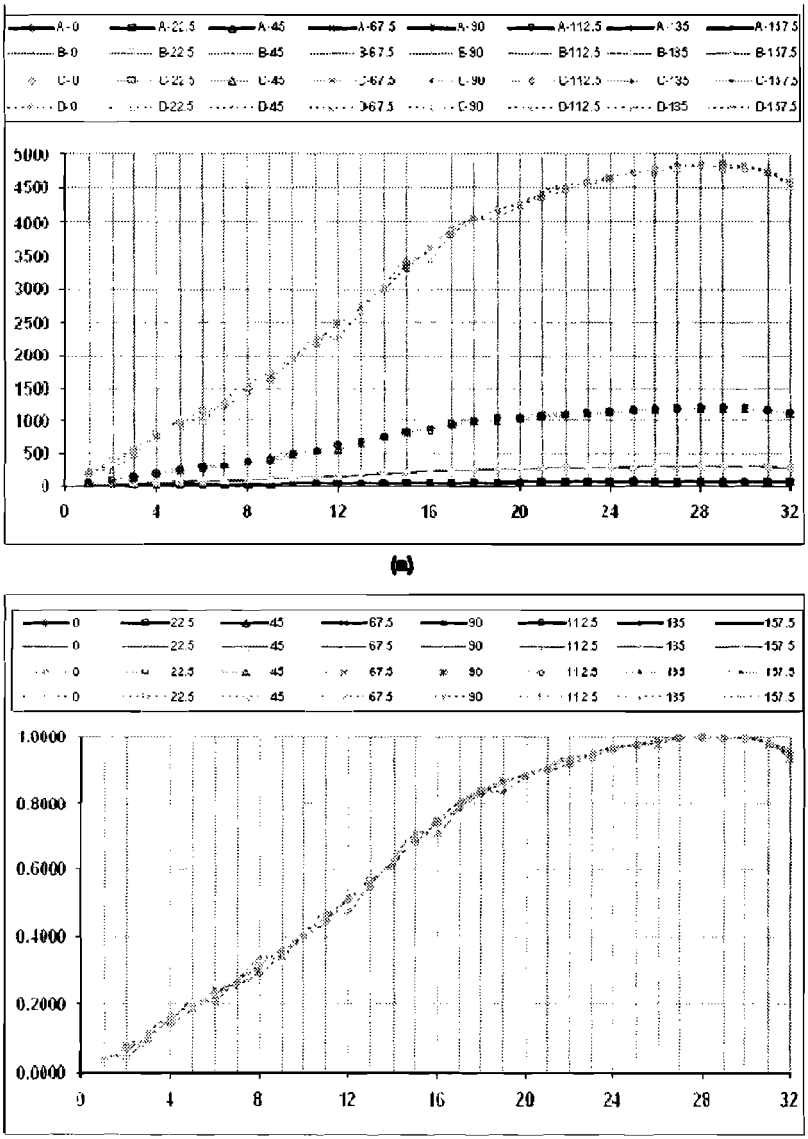

Figure 11. The ratio (%) of standard deviation to mean of the semivariances of 4 image segments in Figure 9 along 8 directions and at each lag: (a) comparison of the ratios between the absolute and relative variograms; (b) the ratios of the relative variogram in detail.

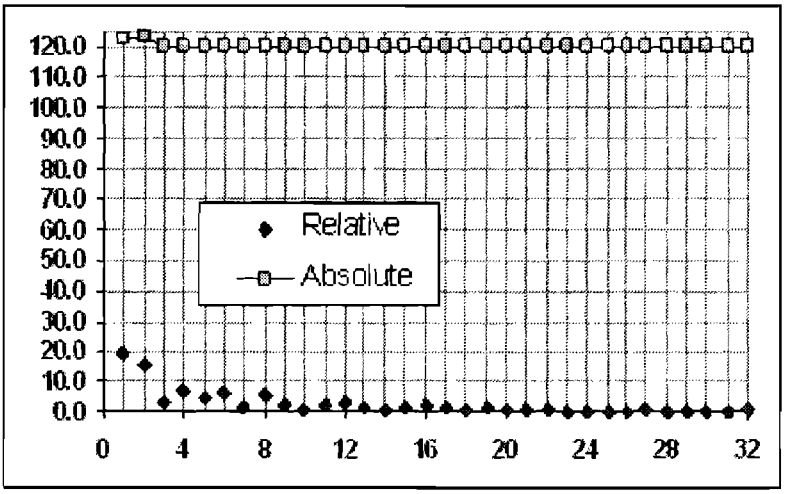

(a)

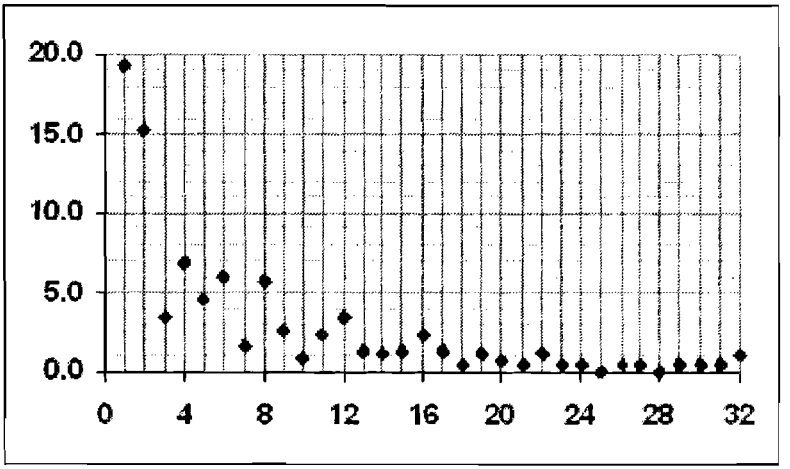

(b)

the ratios derived from the relative semi-variances but in greater detail.

The ratios derived from the absolute semi-variances are extremely high, around 120% for all lags (Fig. 11a). Conversely, the ratios derived from the relative semi-variances are less than 2% for most lags, about a quarter of the lags with a ratio between 2% and 6% (Fig.11b). Only a few lags have ratios larger than 6%, all of which are at extremely short lag distances. The large deviation of ratios at the short lags can be possibly attributed to nugget effects. Nevertheless, the relative variograms for the four image segments are very close, witnessing the ability of relative variograms to characterize equivalent spatial structure regardless of underlying DN value variation.

Conclusions

A series of experiments are conducted to investigate several important issues concerning the appropriate use of variogram-based feature vectors for CBIR. It is argued that except horizontal and vertical directions, lag tolerance and/or directional tolerance are needed to produce semivariances at the same set of lag distances as those readily available along horizontal and vertical directions. For diagonal directions, only a lag tolerance is needed. For other directions, a directional tolerance and a bandwidth should be also set. It is also emphasized that Euclidean distance should always be adopted to avoid adding false anisotropy information not inherent in image objects. The experiments also suggest that, although a square segment is often the convenient and common choice, a circle segment is more appropriate for characterizing the directional spatial continuity of an object contained within an image segment. In addition, relative variograms are more appropriate to represent spatial structure than absolute variograms. In conclusion, although variograms based feature vector can be valuable for characterizing texture and structure information, a proper use of variograms guided by the findings in this paper may better unleash the power of this technique and aid our understanding and interpretation of the results obtained.

References

Aksoy, S., and R.M. Haralick, 2000. Using Texture in Image Similarity and Retrieval, *Texture Analysis in Machine Vision* (M. Pietikainen, editor), World Scientific, Hackensack, NJ, pp.129-149.

Atkinson, P.M., and Lewis, P. (2000). Geostatistical classification for remote sensing: an introduction. *Computers & Geosciences*, 26 (4), 361-371.

Bian, L., 2003. Retrieving urban objects using a wavelet transform approach, *Photogrammetric Engineering and Remote Sensing*, 69(2): 133-141.

Bian, L., and Xie, Z. (2004), A spatial dependence approach to retrieving industrial complexes from digital images. *The Professional Geographer*, 56(3), 381-393.

Carr, J.R. (2002). *Data Visualization in the Geological Sciences*. Upper Saddle River, NJ: Prentice Hall.

Curran, P. (1988). The semivariogram in remote sensing: an introduction. *Remote Sensing of Environment*, 24 (3), 493-507.

Deutsch, C.V, and Journel, A.G. (1997). GSLIB: geostatistical software library and user's guide. New York : Oxford University Press.

Huang, J., R. Kumar, M. Mitra, W. Zhu, and R. Zabih, 1999. Spatial color indexing and applications, *International Journal of Computer Vision*, 35(3): 245-268.

Isaaks, E.H., and Srivastava, R.M. (1989). *Applied Geostatistics*. New York: Oxford University Press.

Jensen, J.R. (2004). *Introductory Digital Image Processing: A Remote Sensing Perspective*. Upper Saddle River, NJ: Prentice Hall.

Jupp, D.L.B., Strahler, A.H., and Woodcock, C.E. (1988). Autocorrelation and regularization in digital images: I. basic theory. *IEEE Transactions on Geoscience and Remote Sensing*, 26 (4), 463-473.

Lark, R.M. (1996). Geostatistical description of texture on an aerial photograph for discriminating classes of land cover. *International Journal of Remote Sensing*,17 (11), 2115-2133.

Miranda, F.P., MacDonald, J.A., and Carr, J.R. (1992). Application of the semi-variogram textural classifier (STC) for vegetation discrimination using SIR-B data of Borneo. *International Journal of Remote Sensing*, 13 (12), 2349-2354.

Pannatier, Y. (1996). VARIOWIN: Software for Spatial Data Analysis in 2D. New York : Springer-Verlag.

St-Onge, B.A., and Cavayas, F. (1995). Estimating forest structure from high resolution imagery using the directional variogram. *International Journal of Remote Sensing*, 16 (11), 1999-2021.

Wallace, C.S.A., Watts, J.M., and Yool, S.R. (2000). Characterizing the spatial structure of vegetation communities in the Mojave Desert using geostatistical techniques. *Computers & Geosciences*, 26 (4), 397-410.

Xie, Z. (2004). A rotation- and flip-invariant algorithm for representing spatial continuity information of geographic images in content-based image retrieval. *Computers & Geosciences*, 30(9/10), 1093-1104.